Electronic Supplementary Information

A heterostructured WO_3-SnO_2 nanocomposite for efficient photocatalytic production of H_2O_2 under visible light

Diya Xie[a], Chen Chen[a], Yaru Wang[a], Cheng Sun[a], Yiming Xu[a,b,*] and Jianguo Huang[a,*]

[a] *Department of Chemistry, Zhejiang University, Hangzhou 310058, PR China*

[b] *State Key Laboratory of Silicon Materials, Zhejiang University, Hangzhou 310027, P.R. China*

*Corresponding author. E-mail address: jghuang@zju.edu.cn (J. Huang).

Contents **pages**

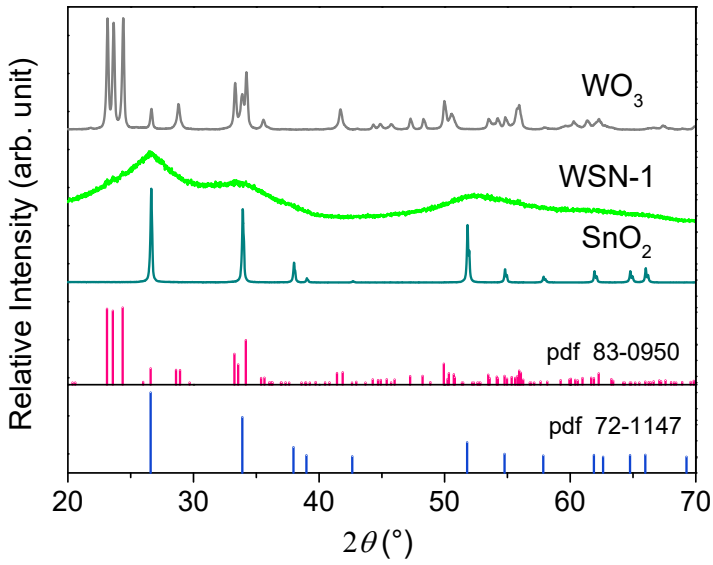

Fig. S1 XRD patterns of WO_3, WSN-1 and SnO_2.

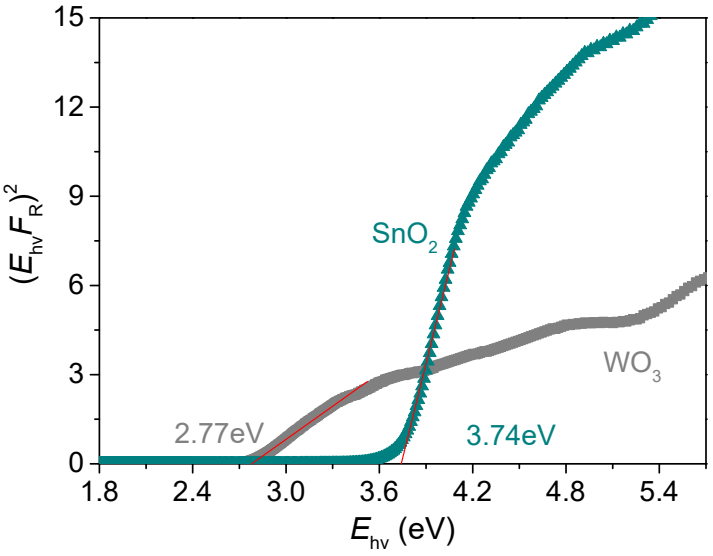

Fig. S2 The direct band gap energy of WO_3 and SnO_2 from Tauc plot, where E_{hv} is light energy, and F_R is Kubella-Munk unit.

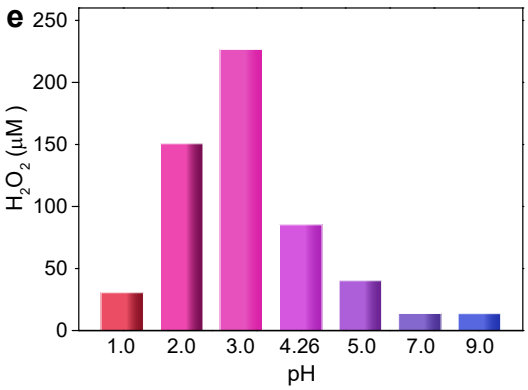

Fig. S3 [H_2O_2] at 5h with different initial pHs (pH was adjusted by droping 0.1 M $HClO_4$ solution before light illumination)

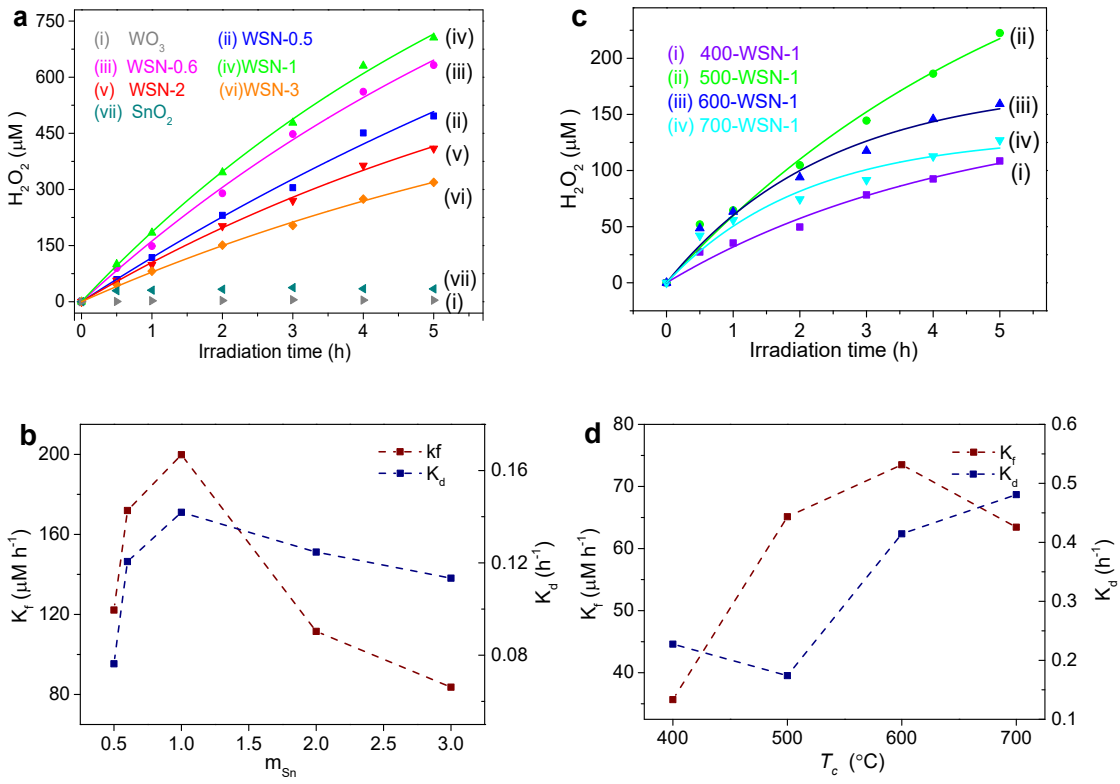

Fig. S4 (a) Production of H_2O_2 on (i) WO_3, (ii) WSN-0.5, (iii) WSN-0.6, (iv) WSN-1, (v) WSN-2, (vi) WSN-3 and (vii) SnO_2 under UV light. (b) The corresponding formation (k_f) and decomposition (k_d) kinetic plots of WSN-*x*. (c) Production of H_2O_2 on T_c-WSN-1 under visible light, T_c = (i) 400℃, (ii) 500℃, (iii) 600℃ and (iv) 700℃. (d) k_f and k_d kinetic plots of T_c-WSN-1.

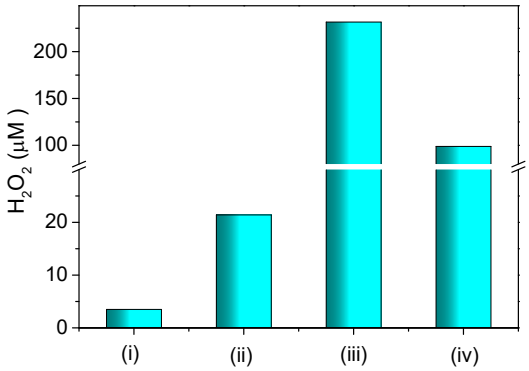

Fig. S5 [H_2O_2] at 5h on WSN-1 (f) in presence of (i) no additive, (ii) 20% methanol, (iii) 20% ethanol, (iv) 20% isopropanol.

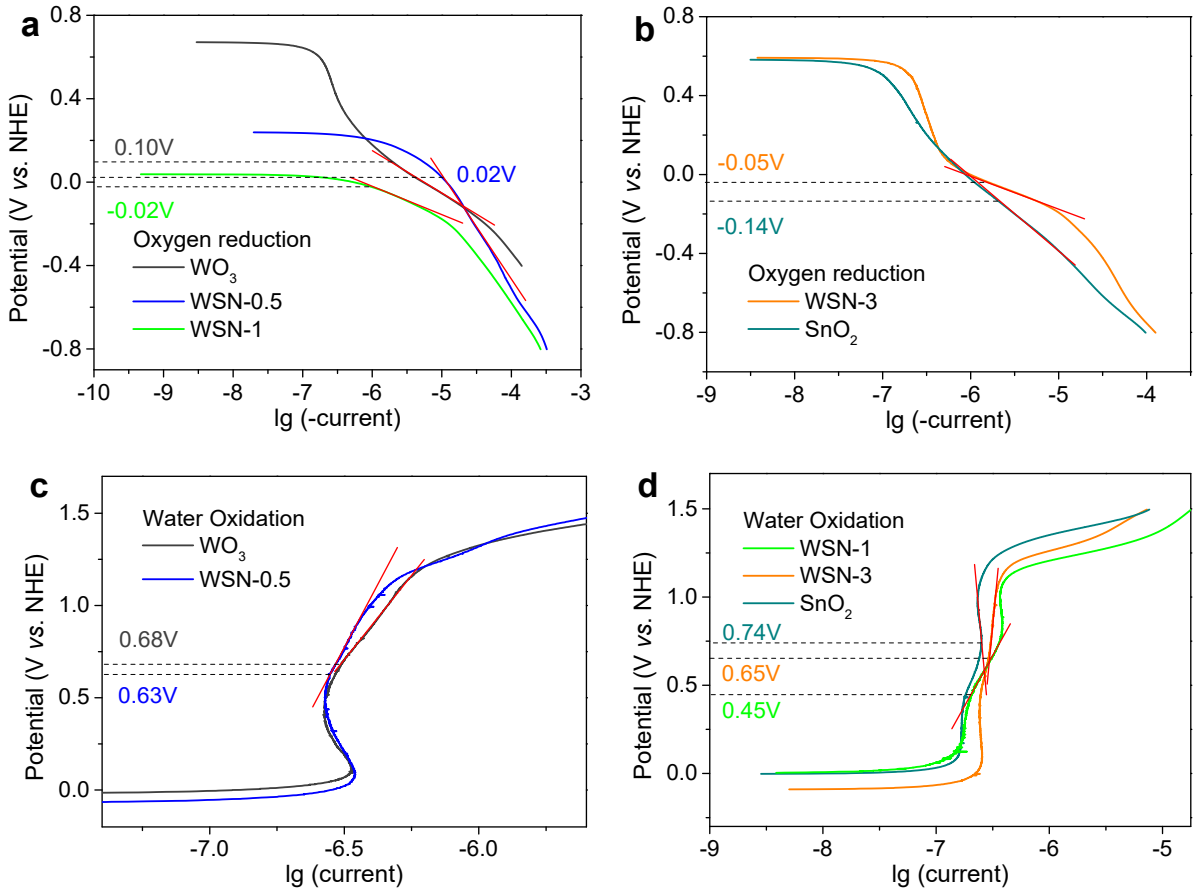

Fig. S6 Curve fitting for the onset potentials of oxygen reduction (a,b) and water oxidation (c,d) in the dark of WO_3, WSN-0.5, WSN-1, WSN-3 and SnO_2.

.

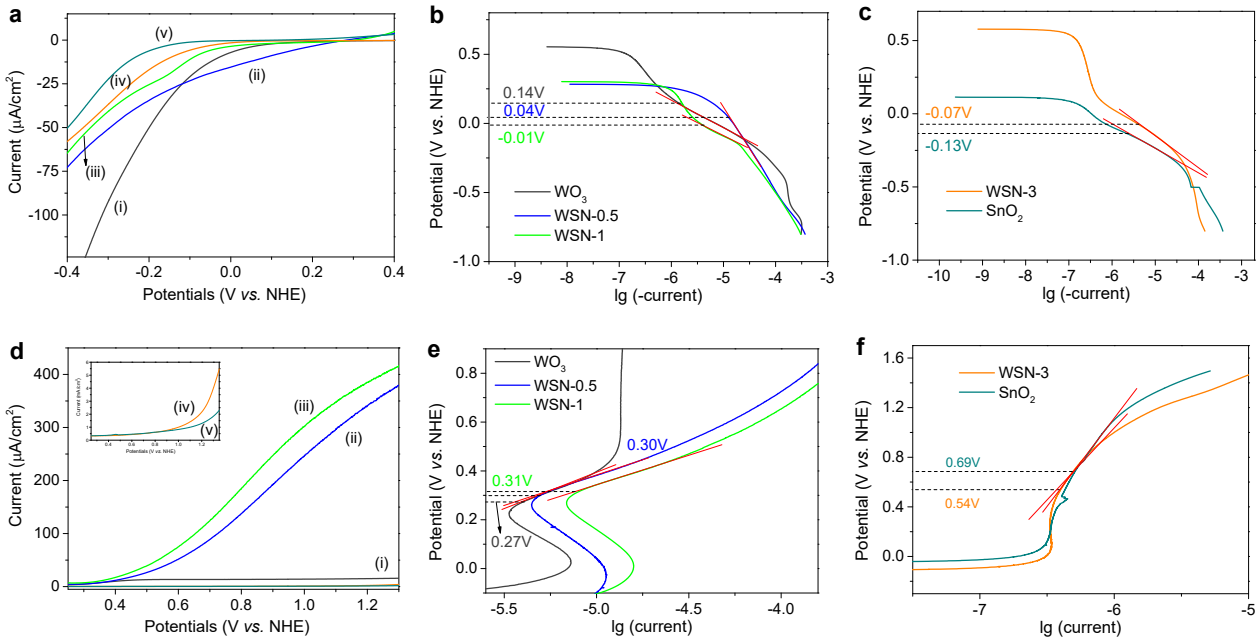

Fig. S7 Light current–voltage curves (a,d) and curve fitting for the onset potentials of oxygen reduction (b,c) and water oxidation (e,f) of (i) WO_3, (ii) WSN-0.5, (iii) WSN-1, (iv) WSN-3 and (v) SnO_2, measured in 0.5 M $NaClO_4$ under O_2 and N_2, respectively.

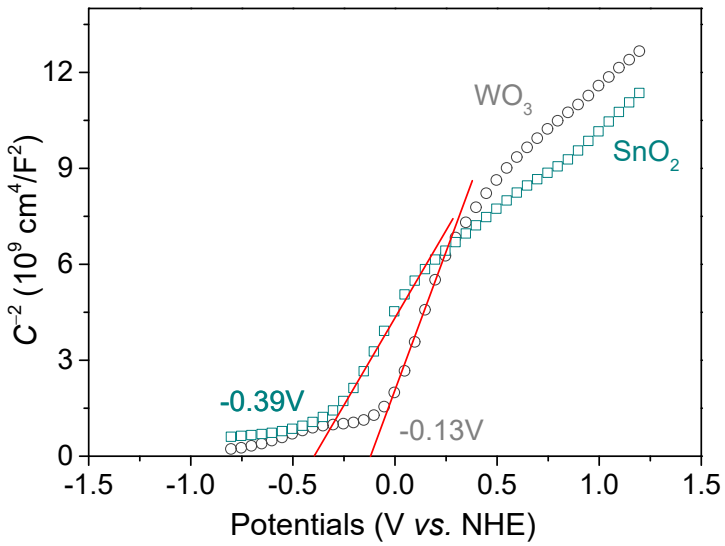

Fig. S8 Mott–Schottky plots for film electrodes of WO_3 and SnO_2, measured at 1 kHz in 0.5 M $NaClO_4$ under N_2.

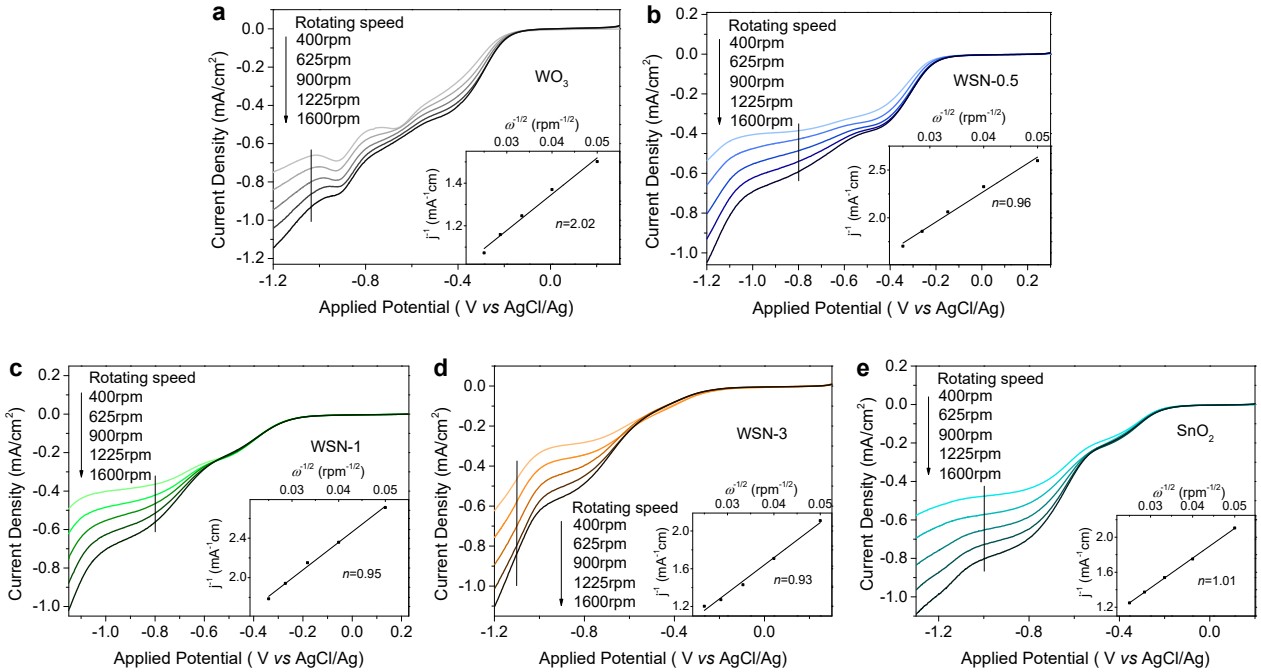

Fig. S9 Dark oxygen reduction of (a) WO_3, (b) WSN-0.5, (c) WSN-1, (d) WSN-3 and (e) SnO_2 on a rotating disk film electrode at different rotating speeds (ω), measured in 0.5 M $NaClO_4$. The average number of electrons (n) for O_2 reduction was calculated from Koutecky-Levich equation, $j^{-1} = j_k^{-1} + B^{-1}\omega^{-1/2}$, and $B = 0.2nFv^{-1/6}CD^{2/3}$,where j is the current, j_k is the kinetic limited current, F is Faraday constant, v the is the kinetic viscosity of water (0.01 cm^2/s), C is O_2 concentration (1.2 μM), and D is O_2 diffusion coeddicient (1.4×10^{-5} cm^2/s).

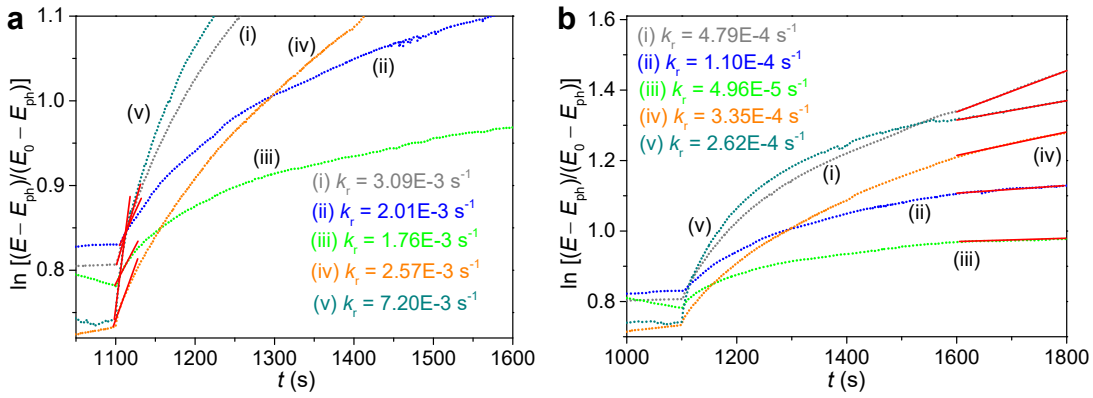

Fig. S10 (a,b) Curve fitting for light off open circuit potentials (OCP) of (i) WO_3, (ii) WSN-0.5, (iii) WSN-1, (iv) WSN-3 and (v) SnO_2. Equation of $(E - E_{ph})/(E_0 - E_{ph}) = 1 - \exp(-k_r t)$ is used, where E is OCP at time t, E_0 and E_{ph} are dark and light stationary OCP, respectively. k_r is the recombination rate constant (J. Kim, D. Monllor-Satoca, W. Choi, Simultaneous production of hydrogen with the degradation of organic pollutants using TiO_2 photocatalyst modified with dual surface components, Energy Environ. Sci. 5 (2012) 7647–7656).

Table S1. The binding energies and percentage of different O species for WSN-*x* samples

Samples	W $4f_{7/2}$	W $4f_{5/2}$	Sn $3d_{5/2}$	Sn $3d_{3/2}$	O_{lat}	O_{abs}
WO_3	35.49	37.63			530.3 (86.7%)	531.3 (13.3%)
SnO_2			486.78	495.21	530.7 (75.6%)	532.1 (24.4%)
WSN-0.5	35.90	38.05	487.17	495.60	530.8 (71.6%)	531.8 (28.4%)
WSN-0.6	35.99	38.13	487.20	495.62	530.9 (71.3%)	532.1 (28.7%)
WSN-1	36.01	38.15	487.27	495.68	530.7 (70.9%)	531.9 (29.1%)
WSN-2	36.16	38.31	487.35	495.74	531.1 (71.6%)	532.1 (28.4%)
WSN-3	36.17	38.31	487.35	495.75	531.1 (72.7%)	532.4 (27.3%)

Table S2. Multi-exponential fitting data of TA kinetic curves for WO_3, WSN-1 and SnO_2 samples

Photocatalyst	τ_1 (ps)	$\lvert A_1 \rvert$	τ_2 (ps)	$\lvert A_2 \rvert$	τ_3 (ps)	$\lvert A_3 \rvert$	τ_{ave} (ps)
WO_3	0.19	1.74E-1	1.76	9.28E-4	35.29	8.73E-4	0.38
WSN-1	0.22	4.24E-3	4.26	1.79E-3	55.89	1.13E-3	10.03
SnO_2	0.14	32.2	1.70	5.28E-4	37.21	1.58E-4	0.14

Table S3. Electrochemical test data for WO_3, SnO_2 and WSN-*x* samples[a]

Samples	E_{on} (V, NHE)		E^b_{on} (V, NHE)		I (uA/cm^2)		I^b (uA/cm^2)	
	ORR	WOR	ORR	WOR	ORR	WOR	ORR	WOR
WO_3	0.10	0.68	0.14[b]	0.27[b]	139.0	0.88	149.0[b]	15.8[b]
WSN-0.5	0.02	0.63	0.04[b]	0.30[b]	66.9	0.93	72.8[b]	379[b]
WSN-1	-0.02	0.45	0.01[b]	0.32[b]	41.5	4.5	64.6[b]	417[b]
WSN-3	-0.05	0.65	-0.07[b]	0.54[b]	29.1	1.67	58.0[b]	4.0[b]
SnO_2	-0.14	0.74	-0.13[b]	0.69[b]	10.8	0.55	53.3[b]	1.8[b]

[a] ORR, oxygen reduction reaction; WOR, water oxidation reaction; E_{on}, the dark onset potential in 0.5 M $NaClO_4$; I, the dark current for the ORR at –0.40 V (NHE), and for the WOR at 1.3 V (NHE). [b] Measured under light (λ > 420 nm).